The influence of material absorption on the quality factor of photonic crystal cavities

Tao Xu, Mark S. Wheeler, Harry E. Ruda, Mohammad Mojahedi, and J. Stewart Aitchison

Department of Electrical and Computer Engineering, University of Toronto

t.xu@utoronto.ca

Abstract: Accounting for material absorption is very important for developing high quality factor (Q) photonic crystal cavities. However, to our knowledge, there have been very few systematic experimental investigations of its role in such cavities. In this paper, we present detailed experiments to reveal the relationship between Q, material absorption coefficient and field pattern. Modes with different field patterns and materials with different absorption coefficients were tested. We have developed a simple formula to describe the relationship, which can be used to replace time-consuming numerical calculations. The experimental and numerical data agree well with this formula.

OCIS codes: (350.4238)Nanophotonics and photonic crystals;(350.4010)Microwaves

References and links

1. Yoshihiro Akahane, Takashi Asano, Bong-Shik Song, and Susumu Noda, "High-Q photonic nanocavity in a two-dimensional photonic crystal," Nature **425,** 944–947 (2003).
2. Kartik Srinivasan, Paul E. Barclay, Oskar Painter, Jianxin Chen, Alfred Y. Cho, and Claire Gmachl, "Experimental demonstration of a high quality factor photonic crystal microcavity," Appl. Phys. Lett. **83,** 1915–1917 (2003).
3. Takashi Asano, Bong-Shik Song and Susumu Noda, "Analysis of the experimental Q factors ($\sim$ 1 million) of photonic crystal nanocavities," Opt. Express **14,** 1996-2002 (2006).
4. C. F. Wang, R. Hanson, D. D. Awschalom, E. L. Hu, T. Feygelson, J. Yang, and J. E. Butler, "Fabrication and characterization of two-dimensional photonic crystal microcavities in nanocrystalline diamond," Appl. Phys. Lett. **91,** 201112 (2007).
5. C. Kreuzer, J. Riedrich-Möller, E. Neu, and C. Becher, "Design of photonic crystal microcavities in diamond films," Opt. Express **16,** 1632–1644 (2008).
6. E. Chow, A. Grot, L.W. Mirkarimi, M. Sigalas, G. Girolami, "Ultracompact biochemical sensor built with two-dimensional photonic crystal microcavity," Opt. Lett. **29,** 1093–1095 (2004).
7. Mindy Lee and Philippe M. Fauchet, "Two-dimensional silicon photonic crystal based biosensing platform for protein detection," Opt. Express **15,** 4530–4535 (2007).
8. I. Alvarado-Rodriguez and E. Yablonovitch, "Separation of radiation and absorption photonic crystal single defect cavities," J. Appl. Phys. **92,** 6399–6402 (2002).
9. T. Xu, S. Yang, S. V. Nair, and H.E. Ruda, "Nanowire-array-based photonic crystal cavity by finite-difference time-domain calculations," Phys. Rev. B **75,** 125104 (2007).
10. T. Xu, S. Yang, S. V. Nair, and H.E. Ruda, "Confined modes in finite-size photonic crystals," Phys. Rev. B **72,** 045126 (2005).
11. T. Xu, M. S. Wheeler, S. V. Nair, H.E. Ruda, M. Mojahedi, and J. S. Aitchison, "Highly confined mode above the light line in a two-dimensional photonic crystal slab," Appl. Phys. Lett. **93,** 241105 (2008).

#106139 - $15.00 USD Received 9 Jan 2009; revised 12 Mar 2009; accepted 12 Mar 2009; published 1 May 2009

1. Introduction

The quality factor (Q) measures the energy leakage rate of the mode confined inside an optical cavity. For a photonic crystal (PhC) cavity, there can be multiple loss channels, among which, radiation losses at the interface between the cavity and the environment and the loss due to the material imperfections are two important factors. The radiation loss can be reduced drastically by engineering the structures with a "gentle confinement" principle [1, 2]. Therefore, the material absorption remains as the greater limiting factor of Q under many circumstances. For instance, in a ultrahigh Q ($>$ 1 million) PhC cavity, the material absorption loss is comparable to the radiation loss even when a small amount of lossy materials such as one atomic layer of water molecules is adsorbed on the surface of the cavity [3]. The absorption in the nanocrystalline diamond film was suspected to be one reason lowering the Q of a PhC cavity [4, 5]. For optical sensing with reagents introduced inside a high-Q cavity [6, 7], the absorption and scattering of the reagent should be considered in addition to the refractive index change .

The dependence of Q on the material absorption in a PhC cavity has been investigated by several groups [5, 8, 3, 9]. To the best of our knowledge, a numerical method, such as three-dimensional (3D) finite-difference time-domain (FDTD) was extensively used and the formula they developed was not complete. The 3D FDTD method with the inclusion of material absorption by adding an imaginary part to the refractive index of lossy materials can generate a quite accurate estimation of total energy loss (total Q). However it is very time consuming. For the same cavity and mode, each time when the material absorption coefficient changes or the lossy materials relocate to different places inside or on the surface of the cavity, recalculation is needed. In this paper, we extend the investigation in two ways. First, we develop a formula to calculate the energy loss due to material absorption and the total energy loss. The formula needs as input the mode field distribution, lossy material distribution and the absorption coefficient. Although the mode field is to be calculated with a numerical method, such as the 3D FDTD method or a plane wave expansion method, it only needs to be calculated once and can be reused for different lossy materials and different lossy material spatial distributions. Second, we compare the prediction from the formula with the results from purely numerical 3D FDTD calculations and experimental results in microwave domain. The prediction from the formula agree well with both the numerical and experimental data.

2. Background theory

Assuming that we have a 2D PhC cavity including an absorptive material M, from [5, 8, 3, 9], the total Q of the cavity including both radiation loss and material loss can be expressed as

$$\frac{1}{Q_{tot}} = \frac{1}{Q_{rad}} + \frac{1}{Q_{abs}}, \tag{1}$$

where $1/Q_{rad}$ and $1/Q_{abs}$ account for the loss due to radiation and material absorption respectively. To calculate $1/Q_{abs}$, some have used $1/Q_{abs} = \alpha/k = 2n_i/n_r$ [5, 3, 9], where $k = 2\pi n_r/\lambda$ is the wavevector, $\alpha = 4\pi n_i/\lambda$ is the absorption coefficient of M, and n_i and n_r are the imaginary and real part of the refractive index of M. The above formula for calculating Q_{abs} is valid only when all the electric field energy of the cavity mode is stored in M. In reality, part of the electric field is in low-loss materials and experiences negligible absorption. For instance, in a hole-array based 2D PhC slab cavity, the field is located mostly in the high dielectric and low-loss materials. When the lossy material M adheres to the air pore walls or the slab surface, Q_{abs} cannot be calculated with $1/Q_{abs} = \alpha/k = 2n_i/n_r$ since the majority of the electric field does not overlap with M. The overlapping between the electric field and the lossy materials should

#106139 - $15.00 USD Received 9 Jan 2009; revised 12 Mar 2009; accepted 12 Mar 2009; published 1 May 2009

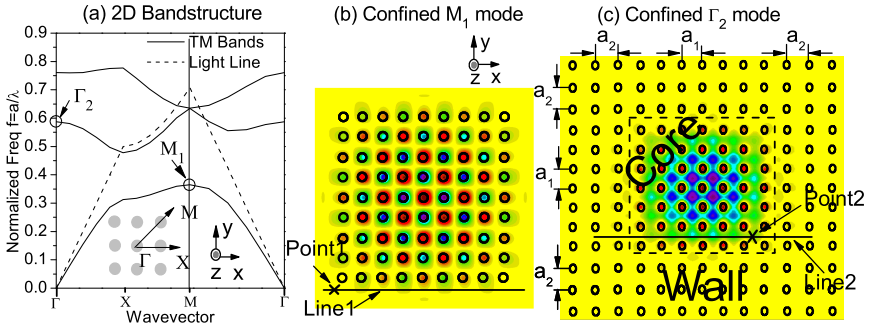

Fig. 1. (a) The 2D bandstructure of a periodic rod array. The refractive index of the rods is 3.122 and the diameter is $0.4a$,where a is the period. (b) A 9×9 array of rods confining M_1 mode. In the microwave experiments, two kinds of dielectric rods are used. In the experiment employing alumina rods, the period a is 4.1 mm and the rods have a diameter D of 1.62 mm and height h of 34.8 mm. When using sapphire rods, $a = 4.4$ mm, $D = 1.74$ mm, and $h = 35$ mm. (c) A heterostructure confining Γ_2 mode. Along the direction perpendicular to the interfaces, the period in the core region a_1 is smaller than the period in the wall region a_2. In the experiment employing alumina rods, a_1 is 8.1 mm, a_2 is 9.7 mm, D is 2.4 mm and h is 47 mm. In (b) and (c), the black circles sketch the outlines of the rods and the E_z field of the confined mode calculated with 3D Finite-Difference Time-Domain (FDTD) overlaps with the structure.

be included and $1/Q_{abs}$ must be written as

$$\frac{1}{Q_{abs}} = Fk/\alpha = 2Fn_i/n_r, \tag{2}$$

$$F = \frac{\int_{V_{abs}} 1/2 \times \varepsilon_r(r)|E(r)|^2 dV}{\int_V 1/2 \times \varepsilon_r(r)|E(r)|^2 dV}, \tag{3}$$

where $\varepsilon_r(r)$ is the real part of the dielectric constant at spatial position r, and F is the filling factor of the electric field energy in the absorptive material M, defined as the ratio between the electric field energy in the absorptive material volume V_{abs} and the total electric field energy in the cavity volume V. In the the numerator part of F, $\varepsilon_r(r)$ is contained in the integration volume V_{abs}. This results in

$$\frac{1}{Q_{tot}} = \frac{1}{Q_{rad}} + 2Fn_i/n_r. \tag{4}$$

To test the validity of the above formula, we considered "photonic" crystal cavities with an array of dielectric rods, constructed for measurement in the microwave spectrum. The material absorption comes from the dielectric rods, whose dielectric properties are well known in the spectral range of the experiments. In the next section, we describe the modes, the cavities, and the experimental setup.

3. Modes and experimental setup

The cavities consist of a square lattice of dielectric rods as shown in Fig. 1. As displayed in the 2D band structure in Fig. 1 (a), two modes were investigated, M_1 and Γ_2, where the letter indicates the crystal wavevector and the number denotes band number. The M_1 mode has most

#106139 - $15.00 USD Received 9 Jan 2009; revised 12 Mar 2009; accepted 12 Mar 2009; published 1 May 2009

of the electric field energy inside the rods, while Γ_2 has half of the electric field energy in air. Two kinds of finite-size cavities were constructed to confine these two modes. A 9×9 array of rods was used to confine the M_1 mode. In the transverse direction, because of the boundary orientation, the mode is "total internally reflected" at the boundary and highly confined as shown in Fig. 1(b) [10]. In the vertical direction, the mode is also highly confined since it is below the light line. The Γ_2 mode is harder to confine since first, it is above the light line and second, no complete band gap exists at that band edge. Therefore, a heterostructure was constructed to confined the Γ_2 mode as show in Fig. 1(c). In the transverse direction, because of the difference in the period, the mode in the core region is in the band gap of the wall region and thus highly confined as shown in the figure. In the vertical direction, we found that Γ_2 mode still satisfies total internal reflection (TIR) conditions even if it is above the light line. All of its planewave components are out of the light cone due to its spatial symmetry. A detailed explanation can be found in Ref. [11].

In the microwave measurements, the rods were supported by two parallel low-loss dielectric sheets (Rogers RT/Duroid 5880 high frequency laminates). A network analyzer (Agilent PNA E8364B) was used to measure the resonance frequency and also the field distribution of the mode. A K-band horn antenna was used as an exciting source and a coaxial monopole antenna was used as a probe. Holes and lines drilled at the top sheet to allow the access of the probing antenna to the field inside the cavity. The reflection coefficient (S_{11}) at port 1 and the transmission coefficient (S_{12}) from port 2 to port 1 were measured. For the gathered data, we used time-gating to remove the early time response, leaving only the long lifetime, high-Q modes. More detailed description of the experimental methods is given elsewhere [11]. The surface roughness and the size fluctuation of the rods were much smaller than the resonance wavelength. In the assembly, the deviation of rod position from the design was also small and the tilting of the rods from the uprightness was negligible. Therefore, all the other loss sources were minimized and only the loss from radiation at the cavity/air interfaces and the material imperfections were significant.

4. Numerical and experimental results

The microwave experiments were carried on with the setup described in the above section. The experimental results are plotted in Fig. 2. Both the frequency spectrum and field patterns are shown for the confined M_1 and Γ_2 modes. The field patterns were measured by assuming the reflection coefficient S_{11} or transmission coefficient S_{12} is proportional to the local field strength. A 3D FDTD calculation including the material absorption was also done. In the calculation, a perfectly matched layer (PML) boundary condition is employed to absorb outgoing waves, and the spatial grid size is $1/16a$, where a is the period of the 9×9 rod array or the core region of the heterogeneous rod array. More details on the FDTD computational method are given in Ref. [10]. By comparing between the measurements and numerical calculations, we could identify the correct frequency peaks corresponding to the confined fundamental M_1 and Γ_2 modes. With these frequency peaks, we can then estimate the experimental $Q_{tot} = \frac{f}{\Delta f}$. Additionally, the field patterns measured confirmed that both modes are highly confined in the cavity both horizontally and vertically, and the M_1 mode confines the electric field more inside the rods, whereas the Γ_2 mode has more electric field in air.

To check the influence of absorption coefficient, we constructed two 9×9 arrays as in Fig. 1(b) with alumina and sapphire rods respectively. Their real refractive indices are similar ($n_r(alumina) = 3.1$ and $n_r(sapphire) = 3.0$), while sapphire rods are less lossy with a smaller imaginary refractive index n_i at about 6.7×10^{-5} than 4.3×10^{-4} of alumina rods. The M_1 modes confined in these two rod arrays have a very close radiation loss ($Q_{rad} \sim 25,000$) and filling factor of about 92% in rods. Therefore, the Q_{tot} is mainly dependent on the absorption

#106139 - $15.00 USD Received 9 Jan 2009; revised 12 Mar 2009; accepted 12 Mar 2009; published 1 May 2009

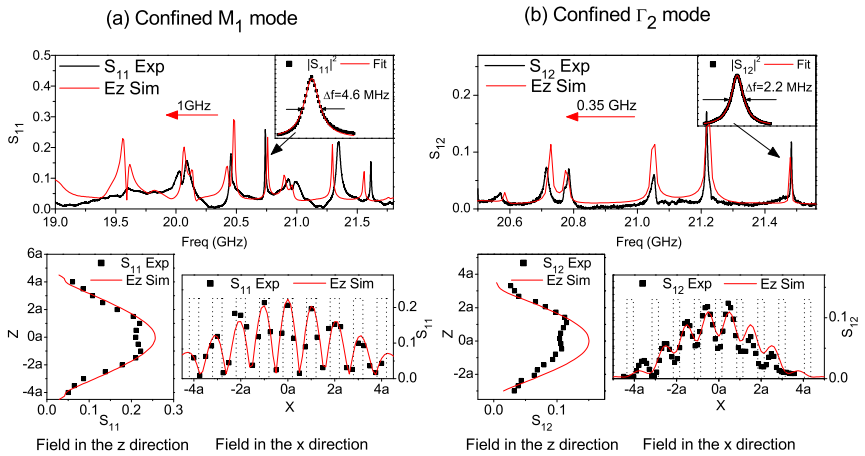

Fig. 2. The comparison between the microwave measurements and 3D FDTD simulation for the confined M_1 mode (a) and Γ_2 mode (b). (Top) Frequency spectrum; (Bottom Left) Field distribution along z direction at Point1(a) and Point2(b); (Bottom Right) Field distribution along Line1(a) and Line2(b), where the dotted columns show the outlines of the rods neighboring the sampling lines. In the frequency spectrum, the simulation curve is shifted to compare with experimental data. Point1, Point2, Line1 and Line2 are marked in Fig. 1(b) and (c). For the data in this figure, alumina rods (Anderman Ceramics) are used in the experiments. In the field distribution figures, *a* in the axis is the period of the PhC.

coefficient, represented by n_i of the rods. For an alumina rod array, Q_{tot} is measured to be about $4,500$, while it is about $14,000$ in a sapphire rod array. With Q_{tot} and Q_{rad}, we can deduce the energy loss due to the material absorption, Q_{abs}, which is about $5,500$ for alumina rods and $32,000$ for sapphire rods . The ratio between $Q_{abs}s$ is roughly the reciprocal of the ratio between n_i of the two materials. To check the influence of the filling factor, a heterogeneous cavity as in Fig. 1(c) consisting of alumina rods was constructed to confine Γ_2 mode. Γ_2 mode has less electric field energy confined in the rods and a smaller filling factor about 50%. Therefore, it experiences less absorption and has a larger measured Q_{tot} of about $9,500$, compared to $4,500$ for the M_1 mode in the 9×9 alumina rod array described above. The deduced Q_{abs} is roughly inversely proportional to the filling factor.

We need to calculate Q_{tot} with Eq. 4 to quantitatively compare with the experimental and numerical results. Firstly, the field pattern and Q_{rad} of the modes were calculated with the 3D FDTD method assuming rods are lossless. The field pattern can then be used to calculate the filling factor F with the knowledge of the rod positions. With Q_{rad}, the filling factor, for each pair of n_r and n_i, Q_{tot} can be derived from Eq. 4. To see the influence of the material absorption, we keep the real part of the refractive index of rods unchanged, while decreasing the imaginary part from a $n_i = n_r/2{,}000$ to $n_i = n_r/2{,}000{,}000$. The Q_{tot} for both M_1 and Γ_2 modes was calculated and are plotted as the two curves in Fig. 3(a). The three experimental points are also shown, which are for M_1 modes in an alumina rod cavity and sapphire rod cavity, and a Γ_2 mode in an alumina rod cavity. As discussed above, with a smaller n_i, the sapphire cavity has a larger Q_{tot} and with a smaller filling factor, the Γ_2 mode tends to have a larger Q_{tot}. The experimental data agree not only qualitatively, but quantitatively with the prediction from Eq. 4. For certain pairs of n_r and n_i, a purely numerical method, i.e., 3D FDTD, was employed to calculate Q_{tot}

#106139 - $15.00 USD Received 9 Jan 2009; revised 12 Mar 2009; accepted 12 Mar 2009; published 1 May 2009

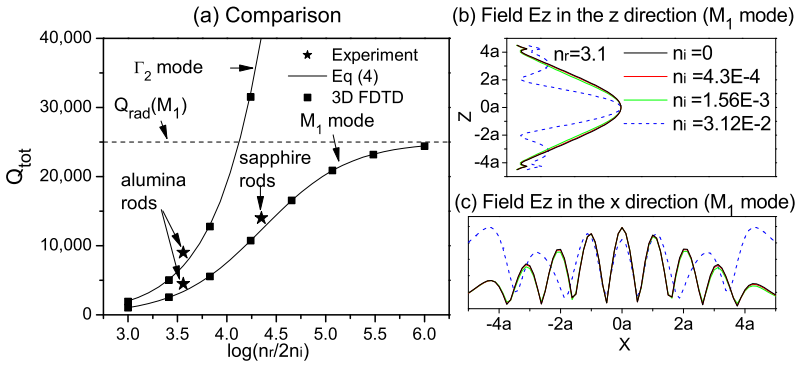

Fig. 3. (a) The comparison between the prediction of Eq. 4 and the numerical and experimental data for the Q of a confined M_1 and Γ_2 mode in dielectric rod cavities. (b) The vertical cross section and (c) the horizontal cross section of the M_1 mode confined in a 9×9 dielectric rod array with different loss levels. For (b) and (c), the geometric data of the cavity and the position of the cross sections are given in Fig. 2(a).

and the results were plotted in the same figure. We can see the prediction of Eq. 4 follows closely the pure numerical data for both high filling factor M_1 mode and low filling factor Γ_2 mode. The excellent agreement in the figure is because we only consider relatively low material losses, where the imaginary refractive index n_i is more than two thousand times smaller than the real part n_r. We have plotted the vertical and horizontal cross sections of the fundamental mode field in the cavities with different material loss levels in Fig. 3(b) and (c). As shown in the figures, for the low material losses, the mode profile is almost identical in the cavity with loss or the cavity without loss. In such a case, the mode field calculated without loss can be used to calculate the filling factor of the mode in cavities with loss. The difference is negligible and our model is valid, as verified in Fig. 3(a). Nevertheless, as the material loss increases to a high level, Q_{abs} will dominate, leading to the broadening of the mode frequency peaks. At certain high level of loss, the neighboring modes will mix, resulting in a different profile from the one without loss. As depicted in dash line in Fig. 3(b) and (c), for the M_1 mode confined in a 9×9 rod array, when n_i is about one hundredth of n_r and the Q_{abs} is about 50, the mode profile deviates from the one without loss greatly. In such a case, our model is no longer valid.

5. Conclusion

A simple formula including the overlap between the electric field and the lossy materials was developed to describe the energy loss of a mode due to material absorption inside a photonic crystal cavity. The prediction of the formula agrees well with the numerical data for low loss materials. Experimental results also confirmed its validity. Since the formula only needs limited numerical calculation, it will greatly help the researchers in the field of photonic crystal cavities to estimate the influence of lossy materials with different level of absorption coefficient and different possible locations.

Acknowledgments

We gratefully acknowledge financial support from NSERC, CIPI, OCE, CSA, AFOSR and ECTI.

#106139 - $15.00 USD Received 9 Jan 2009; revised 12 Mar 2009; accepted 12 Mar 2009; published 1 May 2009